Optics Letters

Giant enhancement of Faraday rotation due to electromagnetically induced transparency in all-dielectric magneto-optical metasurfaces

Aristi Christofi,[1] Yuma Kawaguchi,[1,2] Andrea Alù,[1,3,4,5] and Alexander B. Khanikaev[1,*]

[1]Department of Electrical Engineering, City College of The City University of New York, 160 Convent Ave., New York, New York 10031, USA
[2]Toyohashi University of Technology, 1-1 Hibari-Ga-Oka, Tempaku-cho, Aichi-ken 441-8580, Japan
[3]Photonics Initiative, CUNY Advanced Science Research Center, New York, New York 10031, USA
[4]Physics Program, Graduate Center, City University of New York, New York 10016, USA
[5]e-mail: aalu@gc.cuny.edu
*Corresponding author: akhanikaev@ccny.cuny.edu

Received 18 January 2018; revised 12 March 2018; accepted 13 March 2018; posted 15 March 2018 (Doc. ID 320060); published 11 April 2018

In this Letter we introduce a new class of Fano-resonant all-dielectric metasurfaces for enhanced, high figure of merit magneto-optical response. The metasurfaces are formed by an array of magneto-optical bismuth-substituted yttrium iron garnet nano-disks embedded into a low-index matrix. The strong field enhancement in the magneto-optical disks, which results in over an order of magnitude enhancement of Faraday rotation, is achieved by engineering two (electric and magnetic) resonances. It is shown that while enhancement of rotation also takes place for spectrally detuned resonances, the resonant excitation inevitably results in stronger reflection and low figure of merit of the device. We demonstrate that this can be circumvented by overlapping electric and magnetic resonances of the nanodisks, yielding a sharp electromagnetically induced transparency peak in the transmission spectrum, which is accompanied by gigantic Faraday rotation. Our results show that one can simultaneously obtain a large Faraday rotation enhancement along with almost 100% transmittance in an all-dielectric metasurface as thin as 300 nm. A simple analytical model based on coupled-mode theory is introduced to explain the effects observed in first-principle finite element method simulations.

OCIS codes: (160.3820) Magneto-optical materials; (260.2110) Electromagnetic optics; (310.6628) Subwavelength structures, nanostructures.

https://doi.org/10.1364/OL.43.001838

Magneto-optical (MO) materials and effects have an indispensable role in photonic applications due to their wide use in nonreciprocal devices such as circulators and isolators. However, due to the weak character of MO effects in the optical domain, the footprint of such devices cannot be immediately reduced to the scale compatible with current optical components and integrated optical circuitry. It is therefore a crucial goal to enhance the MO response of naturally occurring materials and achieve MO effects sufficient for practical applications on a micro- and nanoscales. One possible configuration of interest for nonreciprocal devices is Faraday geometry, in which an incident light propagates through an MO material along the direction of its magnetization, and which has been used to achieve optical isolation [1–3] and magnetically induced polarization control.

In thin unpatterned magnetic films the Faraday rotation is proportional to the film thickness and is quite weak. To overcome this problem planar photonic structures referred to as metasurfaces and patterned on nanoscale are very promising solutions. The deliberately designed resonances of metasurfaces can enhance the electromagnetic (EM) field in the MO active region, and, therefore, may allow us to achieve Faraday rotation angles comparable to those obtained in much thicker magnetic films used in isolators.

Indeed, enhanced optical fields have been shown to give rise to larger magneto-optical effects, including Faraday rotation. However, until now, the dielectric designs were mainly based on thick multilayered structures, which inevitably increases the dimensions of the device. As an example, Kato *et al.* [4] studied enhancement of the Faraday effect in a thin film (150-nm thick) of bismuth-substituted yttrium iron garnet (BIG) sandwiched in between two dielectric Bragg mirrors (20 μm each) and confirmed that EM field confinement inside the magnetic defect, which acts like a photonic cavity, results in a 10-fold enhancement of the Faraday rotation, achieving values from 1° to 3°.

Another possible approach to enhance MO response relies on the combination of plasmonic, either guided or localized, and MO properties in thin-film structures [5–7]. An important property of plasmonic nanostructures is associated with their ability to localize light to subwavelength volumes, leading to significant local field enhancement [8]. By embedding MO dielectric inclusions into metallic nanohole arrays [9], or alternatively by placing metallic gratings [10,11], perforated metallic films [12,13], metallic [14,15] or dielectric Mie-resonant nanoparticles [16], or metamaterials [17] in immediate proximity to

MO material, results in significant enhancement of the Faraday rotation and nonreciprocal effects. However, the conditions of high transmittance along with large Faraday rotation, which is crucial for MO devices, is still difficult to achieve due to two factors: (1) loss in metals and (2) resonant reflection.

In recent years, all-dielectric nanostructures, and metasurfaces in particular, have become an active topic of research and have been proven to be of great use for practical applications [18–22]. One of the most significant advantages of metasurfaces stems from the possibility to achieve unique optical responses in subwavelength-thick structures. Such interesting applications as modified Snell's law and flat optical lenses, polarizers, and mode converters, have been demonstrated with structures as thin as several tens of nanometers [23]. Putting all-dielectric metasurfaces in the context of magneto-optics, we expect that, thanks to the possibility to confine and enhance electromagnetic field in metasurfaces, one can achieve strong enhancement of magneto-optical effects in ultrathin films, at the same time avoiding the effects of loss present in plasmonic structures. Indeed, arrays of high-index dielectric nanoparticles are known to support Mie resonances [24–28] and therefore open a path for applications of metamaterials [29], metasurfaces [30–33], and more recently the EIT [34] and Huygens metasurfaces [35], which demonstrate enhanced transmission due to the spectral overlap of electric and magnetic dipole resonances.

The ability to localize the EM field in all-dielectric ultrathin nanostructures generates the interest to investigate all-dielectric MO configurations, consisting of high-index magnetic materials that provide the opportunity to combine MO activity along with Mie resonances [16,36].

In the present work we investigate an all-dielectric MO metasurface consisting of an array of BIG nanodisks embedded into a low-index (SiO_2) matrix with the use of the finite element method. Our results show that we can obtain a large Faraday rotation enhancement along with high transmittance, simultaneously, due to electromagnetically induced transparency (EIT) of the metasurface, for the first time in an all-dielectric nanostructure. The EIT regime is achieved due to the constructive interference of the magnetic and electric dipole resonances, when the structure is optimized in such a way that the two resonances overlap spectrally. We also present a simple analytical model based on coupled mode theory which can provide simple qualitative and quantitative descriptions of the observed effect.

The structure under study is a metasurface of high-index MO disks arranged into a square array embedded into a low-index matrix. The MO dielectric material is magnetized by DC magnetic field along the z direction, and its permittivity has the form $\hat{\epsilon} = [\epsilon, i\epsilon_g, 0; -i\epsilon_g, \epsilon, 0; 0,0,\epsilon]$. This material is assumed to be BIG [37], which is not very dispersive and has the tensor components $\epsilon = 6.25$ and $\epsilon_g = 0.06$ in the frequency range of interest in the DC field of saturation magnetization of ≈0.05 T. The disks are embedded into silica, which has $\epsilon_h = 2.10$. Note that the AC magnetic field of the wave does not magnetize the MO material and does not affect its dielectric properties. However, it does couple with the in-plane magnetic-dipole moments of the MO disks.

Fabrication of the proposed structure can be done by patterning garnet with standard lithography and etching techniques [38], and subsequent deposition of a thick layer of silica or other dielectric with close permittivity. The period of the metasurface, a, is fixed to 850 nm, and the height of the nanodisks, h, is equal to 260 nm. The diameter, D, of the nanodisks is changing depending on the case we are studying and is equal to 720 nm for spectrally separated magnetic and electric resonances and 620 nm for the case of EIT (overlapping resonances). The metasurfaces are illuminated at normal incidence ($\mathbf{k} = k_z\hat{\mathbf{z}}$), and the polarization is chosen along the x direction.

It is worth mentioning here that the choice of the circular shape of the disks and of the square geometry of the lattice is dictated by the symmetry requirement for maximizing the Faraday rotation. Indeed, the conversion of incident linear x-polarization into the orthogonal y-polarization can be efficient only when the x and y polarized modes of the metasurfaces are degenerate. This condition can be easily satisfied by making the disks circular and ensuring that interaction between them is the same in the x and y directions, which is easily achieved by choosing a square array.

In Fig. 2 we first show the results for the case of the metasurface in Fig. 1, which corresponds to the case of spectrally separated magnetic ($\lambda_{mag} = 1429.5$ nm) and electric ($\lambda_{el} = 1456.1$ nm) dipole resonances. Figure 2(a) shows the transmittance, where one can see two well-separated resonances, and, as indicated by their bandwidth, possessing different lifetimes. The inspection of the field profiles in the upper panel in Fig. 2(a) confirms that the modes are indeed dominated by electric and magnetic dipoles and also shows that the field is strongly confined in the MO disks. We also plot the corresponding Faraday rotation angle, θ, in Fig. 2(c) and a trade-off between the transmittance and the rotation angle, a figure of merit (FOM) defined as FOM $= \sqrt{T}|\theta|$ [9,13,39], in Fig. 2(d).

As expected, the field localization in MO disks leads to enhanced MO response and large Faraday rotations, which can reach values of 4 and 1 deg for magnetic and electric resonances, respectively. However, inspection of the FOM appears to be significantly suppressed by the resonant reflection, thus diminishing the benefits of the enhanced Faraday effect. To circumvent this problem, we optimize the structure so that the spectral position of the two resonances is tuned to overlap, leading to Fano resonance and EIT regimes. The tuning is achieved by changing either the diameter D or the height h

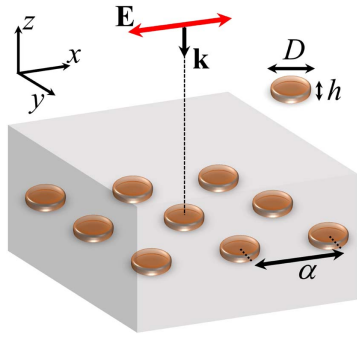

Fig. 1. Structure under consideration: MO nanodisk arrays embedded into a low-index matrix. The MO material is assumed to be BIG and the surrounding medium silica. The period of the metasurface, a, is fixed to 850 nm and the height of the nanodisks, h, is equal to 260 nm. The diameter, D, of the nanodisks is equal to 720 nm for spectrally separated magnetic and electric resonances and 620 nm for overlapping resonances. The light has normal incidence ($\mathbf{k} = k_z\hat{\mathbf{z}}$) and is polarized along the x direction.

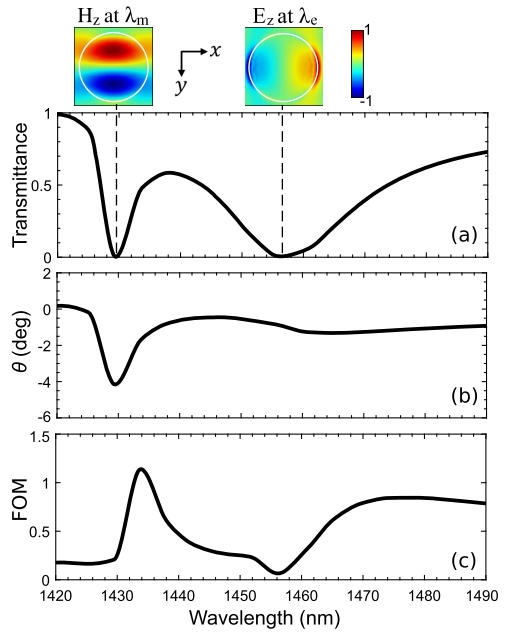

Fig. 2. (a) Transmittance spectrum at normal incidence for the case of two nonoverlapping resonances of magnetic ($\lambda_{\mathrm{mag}} = 1429.5$ nm) and electric ($\lambda_{\mathrm{el}} = 1456.1$ nm) type, for the metasurface of Fig. 1 with $\alpha = 850$ nm, $h = 260$ nm, and $D = 720$ nm. In the margin we also depict the H_z component of the magnetic type resonance and the E_z component of the electric type resonance, both on resonance and at $(0, 0, h)$. (b) Corresponding Faraday rotation angle, θ, of the plane of polarization. (c) FOM between transmittance and rotation angle.

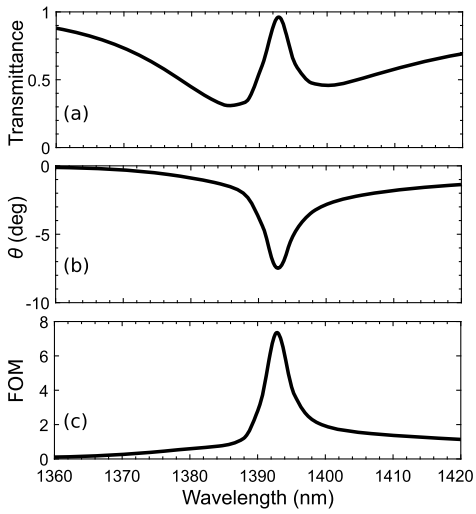

Fig. 3. (a) Transmittance spectrum, at normal incidence, for the case of overlapping resonances at $\lambda = 1392.9$ nm, for the metasurface of Fig. 1 with $\alpha = 850$ nm, $h = 260$ nm, and $D = 620$ nm. (b) Corresponding Faraday rotation angle, θ, of the plane of polarization. (c) FOM between transmittance and rotation angle.

of the nanodisks. We choose to decrease the diameter of the nanodisks so that the resonances overlap at around 1400 nm. Figure 3 shows the finite element method (FEM) simulations results for the case of overlapping resonances. As can be seen, for the modes tuned to match exactly, the constructive interference of the modes takes place at the mid-frequency, leading to a narrow EIT peak of high transmission located between two transmission dips [Fig. 3(a)]. In Fig. 3(b) we present the calculated Faraday rotation angle θ of the transmitted light. As one can see, the combined electric and magnetic dipolar resonant responses lead to even stronger enhancement of Faraday rotation, as large as $\theta = -7.5°$, which is unprecedented for structures as thin as 260 nm. Indeed, in the case of solid BIG film the rotation is $\theta = -0.75°$, and is even lower, $\theta = -0.31°$, if the volume fraction of MO material is the same as in the proposed metasurface, thus yielding over an order of magnitude enhancement. More importantly, the strong Faraday rotation is accompanied by very high transmission, which reached 96% at the EIT peak. Such overlap of high transmission and rotation results in gigantic values of FOM, reaching a maximum value of FOM = 7.35, as shown in Fig. 3(c).

The simulations were performed using the FEM commercial tool COMSOL Multiphysics. Periodic boundary conditions were imposed to reflect the periodic arrangement of the MO disks. Transmission and Faraday rotation were then calculated by direct evaluation in the far field of the zeroth diffraction order (the only propagating order) performing s spatial Fourier transform of the electric field exported from COMSOL to MATLAB.

To interpret the EIT enhanced Faraday rotation, we developed a simple analytical model based on coupled-mode theory (CMT) [40]. The interaction between the incident electric field, $\mathbf{E}^{\mathrm{inc}} = \mathbf{E}_0 e^{i\omega t}$, and two vectorial (two-component) in-plane modes supported by the metasurface (electric, **e**, and magnetic, **m**) can be described by the following CMT equations:

$$\frac{1}{i}\frac{d\mathbf{e}}{dt} = \omega_e \mathbf{e} + \hat{\kappa}_e \mathbf{e} + \alpha_e \mathbf{E}^{\mathrm{inc}}, \tag{1}$$

$$\frac{1}{i}\frac{d\mathbf{m}}{dt} = \omega_m \mathbf{m} + \hat{\kappa}_m \mathbf{m} + \alpha_m \mathbf{E}^{\mathrm{inc}}, \tag{2}$$

where $\omega_{e(m)}$ are complex valued frequencies of electric and magnetic modes (degenerate between x and y dipoles), respectively, $\hat{\kappa}_{e(m)} = [i\kappa_{e(m)}, 0; 0, -i\kappa_{e(m)}]$ are constants describing the polarization conversion of the modes due to the Faraday effect. The parameters $\alpha_{e(m)}$ describe the interaction of the incident field with the electric and magnetic modes, respectively, which can be related to the radiative lifetimes $\tau_{e(m)} = \Im(\omega_{e(m)})^{-1}$ of the modes as $\alpha_{e(m)} = \sqrt{(1/\tau_{e(m)})}$.

The system of Eqs. (1) and (2) can be solved assuming harmonic ($e^{-i\omega t}$) dependence for the incident field and for the modes. Subsequently, the transmitted field can be found through the relation $\mathbf{E}^{\mathrm{tr}} = \hat{t}_0 \mathbf{E}^{\mathrm{inc}} + \alpha_e e^{-i\hat{\phi}_e}\mathbf{e} + \alpha_m e^{-i\hat{\phi}_m}\mathbf{m}$, where $\hat{t}_0$ describes nonresonant transmission through the system and $\hat{\phi}_{e(m)}$ is a diagonal matrix accounting for an additional phase shift in the scattering pathway (e.g., due to retardation). The Faraday rotation angle is found from $\theta = 1/2 \tan^{-1}\{2\Re(\chi)/(1 - |\chi|^2)\}$, where $\chi = E_y^{\mathrm{tr}}/E_x^{\mathrm{tr}}$. Interestingly, the CMT allows for an immediate interpretation of the resonant enhancement as each of the resonant pathways independently leads to the polarization rotation of the scattered field on resonance $\omega = \Re\omega_{e(m)}$ of the form $\theta \approx \kappa_{e(m)}\tau_{e(m)}$ and is proportional to the lifetime of the mode.

In Fig. 4 we plot side-by-side the results of the FEM simulations (black solid lines) and the results of the fitting with the use of the analytical model (red dashed lines). In

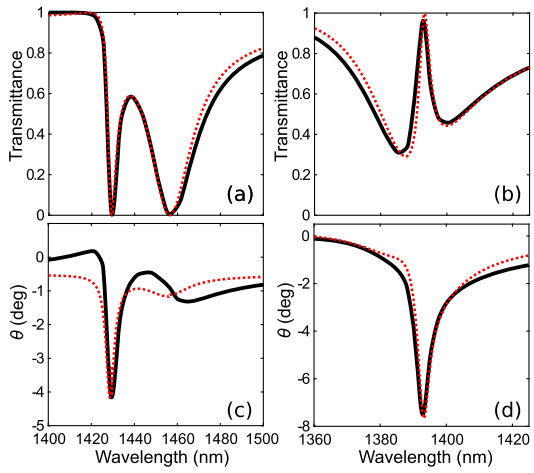

Fig. 4. (a) and (b) Transmittance spectra for the nonoverlapping and overlapping cases of the resonances, respectively. (c) and (d) Corresponding Faraday rotation angles, θ. Black solid lines depict the FEM results and red dashed lines show fitting with the CMT model. The parameters used for fitting in the case of nonoverlapping resonances are $\omega_e = 206$ THz, $\alpha_e = 1.30$ MHz, $\kappa_e = 0.0135$ THz, $\omega_m = 210$ THz, $\alpha_m = 0.580$ MHz, and $\kappa_m = 0.0214$ THz, $t_{xx} = 0.975$, $\phi_{ex} = 1.55\,\pi$ rad, $\phi_{mx} = 1.46\,\pi$rad, $t_{yx} = -0.009$, $\phi_{ey} = 0.557\,\pi$ rad, $\phi_{my} = 0.444\,\pi$ rad. For the case of overlapping resonances: $\omega_e = 216$ THz, $\alpha_e = 1.61$ MHz, $\kappa_e = i0.0865$ THz, $\omega_m = 215$ THz, $\alpha_m = 0.568$ MHz, and $\kappa_m = i0.0323$ THz, $t_{xx} = 0.965$, $\phi_{ex} = 1.55\,\pi$ rad, $\phi_{mx} = 1.47\,\pi$ rad, $t_{yx} = -i0.015$, $\phi_{ey} = 0.605\,\pi$ rad, $\phi_{my} = 0.500\,\pi$ rad.

Figs. 4(a) and 4(b) we show the transmittance spectra for the cases of nonoverlapping and overlapping resonances, respectively. In panels (c) and (d) we show the corresponding results for the Faraday rotation angle θ. As can be seen, our results are in good agreement.

In summary, we introduced highly transmissive all-dielectric MO metasurfaces exhibiting electromagnetically induced transparency for enhanced Faraday rotation. An all-dielectric MO metasurface consisting of BIG nanodisks array embedded into a low-index silica matrix was numerically investigated. We found that a strong Faraday rotation angle is achieved simultaneously with EIT due to the constructive interference of the magnetic and electric dipole resonances. The proposed metasurfaces show great promise for practical applications, offering strong magneto-optical effects in sub-wavelength-thick structures. In addition, large values of the rotation angle envision active optical devices tunable by an external magnetic field.

Funding. National Science Foundation (NSF) (CMMI-1537294, EFRI-1641069); U.S. Department of Energy (DOE) (DE-SC0012704).

Acknowledgment. Research carried out in part at the Center for Functional Nanomaterials, Brookhaven National Laboratory, which is supported by the DOE, Office of Basic Energy Sciences under contract no. DE-SC0012704.

REFERENCES

1. M. Zamani, M. Ghanaatshoar, and H. Alisafaee, J. Opt. Soc. Am. B **28**, 2637 (2011).
2. K. Fang, Z. Yu, V. Liu, and S. Fan, Opt. Lett. **36**, 4254 (2011).
3. S. Chen, F. Fan, X. Wang, P. Wu, H. Zhang, and S. Chang, Opt. Express **23**, 1015 (2015).
4. H. Kato, T. Matsushita, A. Takayama, M. Egawa, K. Nishimura, and M. Inoue, J. Appl. Phys. **93**, 3906 (2003).
5. M. Liu and X. Zhang, Nat. Photonics **7**, 429 (2013).
6. G. Armelles, A. Cebollada, A. García-Martín, and M. U. González, Adv. Opt. Mater. **1**, 10 (2013).
7. I. S. Maksymov, Nanomaterials **5**, 577 (2015).
8. S. A. Maier, *Plasmonics: Fundamentals and Applications* (Springer, 2007).
9. A. B. Khanikaev, A. V. Baryshev, A. A. Fedyanin, A. B. Granovsky, and M. Inoue, Opt. Express **15**, 6612 (2007).
10. V. I. Belotelov, L. L. Doskolovich, V. A. Kotov, E. A. Bezus, D. A. Bykov, and A. K. Zvezdin, Opt. Commun. **278**, 104 (2007).
11. J. Y. Chin, T. Steinle, T. Wehlus, D. Dregely, T. Weiss, V. I. Belotelov, B. Stritzker, and H. Giessen, Nat. Commun. **4**, 1599 (2013).
12. V. I. Belotelov, L. L. Doskolovich, and A. K. Zvezdin, Phys. Rev. Lett. **98**, 077401 (2007).
13. D. Li, L. Chen, C. Lei, J. L. Menendez, C. Mallada, Z. Tang, S. Tang, and Y. Du, J. Opt. Soc. Am. B **33**, 922 (2016).
14. A. V. Baryshev and A. M. Merzlikin, J. Opt. Soc. Am. B **33**, 1399 (2016).
15. E. Almpanis, P. A. Pantazopoulos, N. Papanikolaou, V. Yannopapas, and N. Stefanou, J. Opt. Soc. Am. B **33**, 2609 (2016).
16. M. G. Barsukova, A. S. Shorokhov, A. I. Musorin, D. N. Neshev, Y. S. Kivshar, and A. A. Fedyanin, ACS Photon. **4**, 2390 (2017).
17. S. H. Mousavi, A. B. Khanikaev, J. Allen, M. Allen, and G. Shvets, Phys. Rev. Lett. **112**, 117402 (2014).
18. A. I. Kuznetsov, A. E. Miroshnichenko, M. L. Brongersma, Y. S. Kivshar, and B. Luk'yanchuk, Science **354**, aag2472 (2016).
19. S. Jahani and Z. Jacob, Nat. Nanotechnol. **11**, 23 (2016).
20. B. Bai, J. Tervo, and J. Turunen, New J. Phys. **8**, 205 (2006).
21. D. A. Bykov and L. L. Doskolovich, J. Mod. Opt. **57**, 1611 (2010).
22. F. Fan, S. Chen, W. Lin, Y.-P. Miao, S.-J. Chang, B. Liu, X.-H. Wang, and L. Lin, Appl. Phys. Lett. **103**, 161115 (2013).
23. N. F. Yu and F. Capasso, Nat. Mater. **13**, 139 (2014).
24. J. A. Schuller, R. Zia, T. Taubner, and M. L. Brongersma, Phys. Rev. Lett. **99**, 107401 (2007).
25. J. C. Ginn, I. Brener, D. W. Peters, J. R. Wendt, J. O. Stevens, P. F. Hines, L. I. Basilio, L. K. Warne, J. F. Ihlefeld, P. G. Clem, and M. B. Sinclair, Phys. Rev. Lett. **108**, 097402 (2012).
26. A. B. Evlyukhin, S. M. Novikov, U. Zywietz, R. L. Eriksen, C. Reinhardt, S. I. Bozhevolnyi, and B. N. Chichkov, Nano Lett. **12**, 3749 (2012).
27. I. Staude, A. E. Miroshnichenko, M. Decker, N. T. Fofang, S. Liu, E. Gonzales, J. Dominguez, T. S. Luk, D. N. Neshev, I. Brener, and Y. Kivshar, ACS Nano **7**, 7824 (2013).
28. M. Terakawa, S. Takeda, Y. Tanaka, G. Obara, T. Miyanishi, T. Sakai, T. Sumiyoshi, H. Sekita, M. Hasegawa, P. Viktorovitch, and M. Obara, Prog. Quantum Electron. **36**, 194 (2012).
29. Q. Zhao, J. Zhou, F. Zhang, and D. Lippens, Mater. Today **12**(12), 60 (2009).
30. M. I. Shalaev, J. Sun, A. Tsukernik, A. Pandey, K. Nikolskiy, and N. M. Litchinitser, Nano Lett. **15**, 6261 (2015).
31. F. Fan, S. Chen, and S.-J. Chang, IEEE. J. Sel. Top. Quantum. Electron. **23**, 1 (2017).
32. R. Alcaraz de la Osa, J. M. Saiz, F. Moreno, P. Vavassori, and A. Berger, Phys. Rev. B **85**, 064414 (2012).
33. A. Berger, R. Alcaraz de la Osa, A. K. Suszka, M. Pancaldi, J. M. Saiz, F. Moreno, H. P. Oepen, and P. Vavassori, Phys. Rev. Lett. **115**, 187403 (2015).
34. Y. Yang, I. I. Kravchenko, D. P. Briggs, and J. Valentine, Nat. Commun. **5** 5753 (2014).
35. M. Decker, I. Staude, M. Falkner, J. Dominguez, D. N. Neshev, I. Brener, T. Pertsch, and Y. S. Kivshar, Adv. Opt. Mater. **3**, 813 (2015).
36. A. Christofi, N. Stefanou, and N. Papanikolaou, Phys. Rev. B **89**, 214410 (2014).
37. Z. Yu, Z. Wang, and S. Fan, Appl. Phys. Lett. **90**, 121133 (2007).
38. T. Shintaku, T. Uno, and M. Kobayashi, J. Appl. Phys. **74**, 4877 (1993).
39. C. Lei, L. Chen, Z. Tang, D. Li, Z. Cheng, S. Tang, and Y. Du, Opt. Lett. **41**, 729 (2016).
40. S. Fan, W. Suh, and J. D. Joannopoulos, J. Opt. Soc. Am. A **20**, 569 (2003).